Anisotropic Pseudorotation of the Photoexcited Triplet State of Fullerene C 60 in Molecular Glasses Studied by Pulse EPR

ARTICLE *in* THE JOURNAL OF PHYSICAL CHEMISTRY A · APRIL 2008

Impact Factor: 2.69 · DOI: 10.1021/jp0765291 · Source: PubMed

6 AUTHORS, INCLUDING:

Leonid Kulik
Russian Academy of Sciences
78 PUBLICATIONS **602** CITATIONS
SEE PROFILE

Ruslan Bulatovich Zaripov
Russian Academy of Sciences
17 PUBLICATIONS **31** CITATIONS
SEE PROFILE

Sergei A Dzuba
Russian Academy of Sciences
111 PUBLICATIONS **1,684** CITATIONS
SEE PROFILE

ARTICLES

Anisotropic Pseudorotation of the Photoexcited Triplet State of Fullerene C_{60} in Molecular Glasses Studied by Pulse EPR

Mikhail N. Uvarov,[†] Leonid V. Kulik,[‡] Mikhail A. Bizin,[‡] Valentina N. Ivanova,[£] Ruslan B. Zaripov,[§] and Sergei A. Dzuba*[,†,‡]

Novosibirsk State University, 630090 Pirogova 2, Novosibirsk, Russia, Institute of Chemical Kinetics and Combustion, 630090 Institutskaya 3, Novosibirsk, Russia, Institute of Inorganic Chemistry, 630090 Lavrentjev Ave. 3, Novosibirsk, Russia, and Zavoisky Physical-Technical Institute of RAS, 420029 Sibirskii trakt 10/7, Kazan, Russia

Received: August 14, 2007; In Final Form: December 20, 2007

Spin-polarized echo-detected electron paramagnetic resonance (EPR) spectra and the transversal relaxation rate T_2^{-1} of the photoexcited triplet state of fullerene C_{60} molecules were studied in *o*-terphenyl, 1-methylnaphthalene, and decalin glassy matrices. The model is composed of a fast (correlation time $\sim 10^{-12}$ s) pseudorotation of $^3C_{60}$ in a local anisotropic potential created by interaction of the fullerene molecule with the surrounding matrix molecules. In simulations, this potential is assumed to be axially symmetric around some axis of a preferable orientation in a matrix cage. The fitted value of the potential was found to depend on the type of glass and to decrease monotonically with a temperature increase. A sharp increase of the T_2^{-1} temperature dependence was found near 240 K in glassy *o*-terphenyl and near 100 K in glassy 1-methylnaphthalene and decalin. This increase probably is related to the influence on the pseudorotation of the onset of large-amplitude vibrational molecular motions (dynamical transition in glass) that are known for glasses from neutron scattering and molecular dynamics studies. The obtained results suggest that molecular and spin dynamics of the triplet fullerene are extremely sensitive to molecular motions in glassy materials.

Introduction

Since the discovery of fullerenes, they have attracted much attention because of the unusual physical and chemical properties and because of the possible technical applications of fullerene-based materials.[1] The fullerene C_{60} can be easily excited by visible light, which leads to the formation of the $^3C_{60}$ triplet state, with the quantum yield close to unity. This state is characterized by high electron spin polarization. That is why the fullerene-based materials possibly may be used as an active media for masers.[2]

Previously, the $^3C_{60}$ triplet state was studied by time-resolved electron paramagnetic resonance (EPR),[3−8] optically detected EPR,[9−11] electron spin echo (ESE),[12−15] ^{13}C electron−nuclear double resonance (ENDOR),[16,17] and Fourier transform EPR.[18−20] Several theoretical attempts to calculate and interpret the zero-field splitting (ZFS) parameters of $^3C_{60}$ were undertaken.[21−23] The ZFS parameters were found to slightly depend on the matrix in which the fullerene is embedded.

The $^3C_{60}$ molecule has the shape of a prolate ellipsoid, with the longest axis coinciding with the direction of the *z* axis of the ZFS tensor. A strong narrowing of the $^3C_{60}$ spin-polarized EPR spectrum in molecular glasses was observed with increasing temperature. For interpretation of this narrowing, the concept of rapid pseudorotation (dynamic Jahn−Teller effect) was used.[5−7] The pseudorotation implies the change of the directions of the $^3C_{60}$ principal ZFS axes resulting in the exchange between different $^3C_{60}$ EPR frequencies. In early works,[5−7] pseudorotation was assumed to be fully isotropic, with the principal ZFS for any given molecule acquiring any orientation in the cage with equal probability.

In this paper, we show that the model of isotropic pseudorotation is, however, in apparent contradiction with experimental ESE data on $^3C_{60}$ in molecular glasses. The model of anisotropic pseudorotation is proposed, which is consistent with the whole data sets obtained. Three types of molecular glass formers are studied here, *o*-terphenyl, 1-methylnaphthalene, and decalin.

Theoretical Background

The simulation of the $^3C_{60}$ EPR spectra was based on a well-established theoretical approach.[24−26] The Hamiltonian of an organic molecule in a triplet state is a sum of the Zeeman Hamiltonian and the ZFS Hamiltonian $\mathscr{H}_D$

$$\mathscr{H} = g\beta\mathbf{B_0}\mathbf{S} + \mathscr{H}_D$$

where $\mathbf{B_0}$ is the magnetic field vector, $\mathbf{S}$ is the spin vector ($S = 1$), β is the Bohr magneton, g is the g-factor that for $^3C_{60}$ may be assumed to be isotropic with good accuracy, and $\mathscr{H}_D = (1/$

* To whom correspondence should be addressed. E-mail: dzuba@ns.kinetics.nsc.ru
† Novosibirsk State University.
‡ Institute of Chemical Kinetics and Combustion.
£ Institute of Inorganic Chemistry.
§ Zavoisky Physical-Technical Institute of RAS.

10.1021/jp0765291 CCC: $40.75
Published on Web 02/26/2008

2)$S_iD_{ij}S_j$, where D_{ij} are the components of ZFS tensor. In the framework of the principal axes (x, y, z) of this tensor (referred to below as a molecular framework), the ZFS Hamiltonian has the simple form

$$\mathscr{H}_D = D\left(S_z^2 - \frac{1}{3}\mathbf{S}^2\right) + E(S_x^2 - S_y^2)$$

In the molecular framework $\mathbf{B_0} = B_0(\sin\theta\cos\varphi, \sin\theta\sin\varphi, \cos\theta)$, where θ and φ are, respectively, the polar and the azimuthal angles determining the orientation of the $\mathbf{B_0}$ vector. In the laboratory framework (X, Y, Z), where the Z axis is parallel to the external magnetic field direction, $\mathscr{H}_D$ can be written as

$$\mathscr{H}_D = \frac{1}{2}\left(\frac{D}{3}(3\cos^2\theta - 1) + E\sin^2\theta\cos 2\varphi\right)(3S_Z^2 - \mathbf{S}^2) \quad (1)$$

For $^3C_{60}$ at the X-band EPR, the condition $g\beta B_0 \gg D$ holds (high-field approximation). The energy levels W_+, W_0, and W_- of the three high-field eigenstates T_+, T_0, and T_- are

$$\begin{aligned} W_+ &= g\beta B_0 + \frac{D}{6}(3\cos^2\theta - 1) + \frac{E}{2}\sin^2\theta\cos 2\varphi \\ W_0 &= -\frac{D}{3}(3\cos^2\theta - 1) - E\sin^2\theta\cos 2\varphi \\ W_- &= -g\beta B_0 + \frac{D}{6}(3\cos^2\theta - 1) + \frac{E}{2}\sin^2\theta\cos 2\varphi \end{aligned} \quad (2)$$

The energies of two allowed, $T_0 \leftrightarrow T_+$ and $T_0 \leftrightarrow T_-$, transitions are, respectively

$$\begin{aligned} h\nu_{0+} &= g\beta B_0 + \frac{D}{2}(3\cos^2\theta - 1) + \frac{3E}{2}\sin^2\theta\cos 2\varphi \\ h\nu_{0-} &= g\beta B_0 - \frac{D}{2}(3\cos^2\theta - 1) - \frac{3E}{2}\sin^2\theta\cos 2\varphi \end{aligned} \quad (3)$$

The high-field triplet eigenfunctions T_+, T_0, and T_- can be written through the zero-field eigenfunctions T_x, T_y, and T_z as

$$\begin{aligned} T_+ &= T_x\frac{\mathrm{i}\sin\varphi + \cos\theta\cos\varphi}{\sqrt{2}} - T_y\frac{\mathrm{i}\cos\varphi + \cos\theta\sin\varphi}{\sqrt{2}} + T_z\frac{\sin\theta}{\sqrt{2}} \\ T_0 &= T_x\sin\theta\cos\varphi + T_y\sin\theta\sin\varphi + T_z\cos\theta \\ T_- &= -T_x\frac{\mathrm{i}\sin\varphi + \cos\theta\cos\varphi}{\sqrt{2}} + T_y\frac{\mathrm{i}\cos\varphi + \cos\theta\sin\varphi}{\sqrt{2}} + T_z\frac{\sin\theta}{\sqrt{2}} \end{aligned} \quad (4)$$

From eq 4, it follows that populations p_+, p_0, and p_- of the high-field eigenstates may be expressed via the populations of zero-field eigenstates p_x, p_y, and p_z

$$\begin{aligned} p_+ = p_- &= \frac{1}{2}p_x(\cos^2\theta\cos^2\varphi + \sin^2\varphi) + \frac{1}{2}p_y(\cos^2\theta\sin^2\varphi + \cos^2\varphi) + \frac{1}{2}p_z\sin^2\theta \\ p_0 &= p_x\sin^2\theta\cos^2\varphi + p_y\sin^2\theta\sin^2\varphi + p_z\cos^2\theta \end{aligned} \quad (5)$$

Therefore, the polarizations of two allowed EPR transitions are

$$\begin{aligned} p_0 - p_+ = -(p_- - p_0) = &\frac{1}{2}p_x(2\sin^2\theta\cos^2\varphi - \cos^2\theta\cos^2\varphi - \sin^2\varphi) + \\ &\frac{1}{2}p_y(2\sin^2\theta\sin^2\varphi - \cos^2\theta\sin^2\varphi - \cos^2\varphi) + \\ &\frac{1}{2}p_z(2\cos^2\theta - \sin^2\theta) \end{aligned} \quad (6)$$

Note that these polarizations are of the opposite sign, with one in emission and the other in absorption.

To obtain EPR spectra, the averaging over angles θ and φ must be performed, taking into account also additional broadening due to unresolved hyperfine interactions with surrounding nuclei

$$G_\pm(B_0) = \frac{1}{4\pi}\int\int \sin\theta\,\mathrm{d}\theta\,\mathrm{d}\varphi(\pm p_\pm \mp p_0)f\left(B_0 - \frac{h\nu}{g\beta} \pm B_{\mathrm{ZFS}}\right) \quad (7)$$

where B_0 is the scanning magnetic field, ν is the EPR spectrometer operating frequency, function $f(B)$ describes the line shape induced by unresolved interactions, and

$$B_{\mathrm{ZFS}} = \frac{D}{2g\beta}(3\cos^2\theta - 1) + \frac{3E}{2g\beta}\sin\theta^2\cos 2\varphi \quad (8)$$

The two resulting line shapes $G_\pm(B_0)$ in eq 7 are to be summed.

Experimental Section

Fullerene C_{60} was synthesized and purified according to the method described in ref 27. *o*-Terphenyl (Tokyo Kasei), 1-methylnaphthalene (Soyuzreakhim), and decalin (1:1 mixture of *cis*- and *trans*-decalin, Sigma-Aldrich) were used as solvents. The solvents were distilled. The fullerene was dissolved at a concentration of about 10^{-4} M. The solution was put in glass tubes of a 4 mm inner diameter. Three freeze−pump−thaw cycles were executed, and then, the tubes were sealed under vacuum. The *o*-terphenyl sample prior the measurements was heated up to the melting point and then quickly frozen with liquid nitrogen to obtain a glassy state. The glassy state of the 1-methylnaphthalene and decalin samples was obtained by freezing with liquid nitrogen.

In some experiments, we used stable nitroxide radical **1**

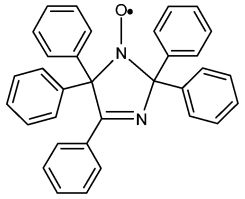

1

which was synthesized and gifted by Professor V. A. Reznikov (Novosibirsk Institute of Organic Chemistry).

Electron spin echo experiments were carried out on an X-band Bruker ESP-380E FT EPR spectrometer equipped with a dielectric cavity (Bruker ER 4118 X-MD-5) inside of an Oxford Instruments CF 935 cryostat. The spectrometer dead time was ~100 ns. A microwave pulse sequence of $\pi/2 - \tau - \pi - \tau -$ echo was used. The echo signal in the time domain was integrated by a built-in spectrometer integrator. The delay after laser flash (DAF) was about 100 ns. Echo-detected EPR spectra

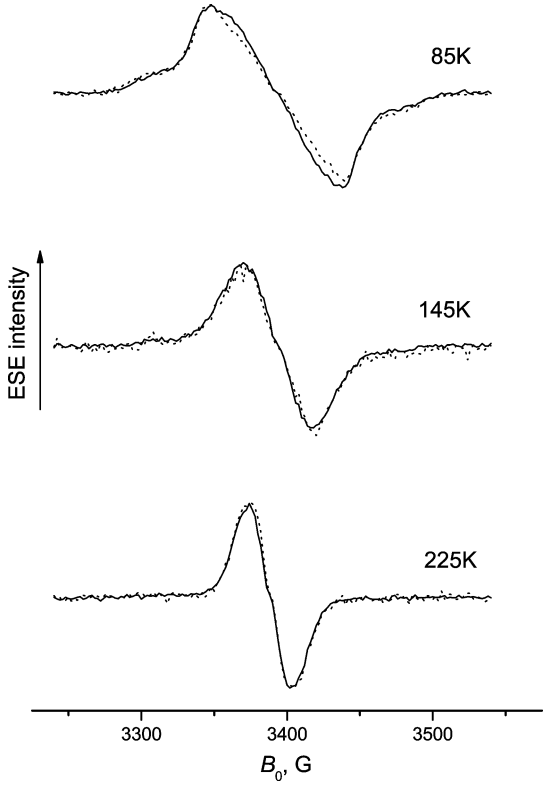

Figure 1. Two-pulse echo-detected EPR spectra of $^3C_{60}$ in *o*-terphenyl glass at three different temperatures obtained at two interpulse delays τ. Solid lines: $\tau = 120$ ns; dotted lines: $\tau = 600$ ns. Spectra are arbitrarily shifted along the vertical axis. Spectra are normalized to the same maximal amplitude to visualize a possible τ dependence of the line shape.

were recorded taken at a fixed τ while scanning the magnetic field. The transversal relaxation rate T_2^{-1} was measured at a constant magnetic field corresponding to the maximum of the spectrum while scanning τ interval.

For photoexcitation of the sample, the second harmonic of a pulsed Nd:YAG laser Surelite I-10 was used, with a wavelength of 532 nm, a pulse duration of 10 ns, a pulse energy of 10 mJ, and a pulse repetition rate of 10 Hz. The temperature was controlled by a cold nitrogen flow and measured with a copper-constantan thermocouple attached to the sample.

For numerical simulation, the MATLAB 7.0 program package was used.

Results and Discussion

Figure 1 shows, for some selected temperatures, the $^3C_{60}$ echo-detected EPR spectra for the *o*-terphenyl sample taken at two different τ delays. One can see that spectra are spin-polarized, with the low-field absorptive part and the high-field emissive one. Spectra are normalized to the same maximal intensity to make visible a possible line shape dependence on τ. One can see that this dependence is negligible. This result implies that transversal relaxation does not influence the experimental EPR line shape, which therefore may be directly compared with the theoretical line shape given by eq 7.

The decay of the $^3C_{60}$ ESE signal with the DAF increase was found, to a good approximation, to be monoexponential for all glasses and temperatures studied (data not shown). The temperature dependence of the rate of this decay k_D is shown in Figure 2. One can see that this rate increases with temperature and it does not noticeably depend on the glass.

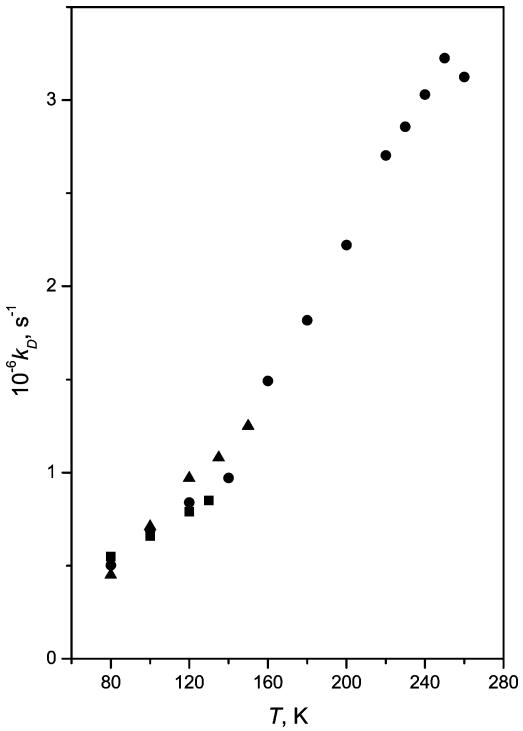

Figure 2. Temperature dependence of the decay rate for the $^3C_{60}$ ESE signal with the DAF increase. Circles: *o*-terphenyl glass; triangles: 1-methylnaphthalene glass; squares: decalin glass. The signal was measured at the EPR spectral position corresponding to the left maximum (see Figure 1).

Experimental echo-detected EPR spectra of $^3C_{60}$ observed at different temperatures are shown as thin lines in Figures 3, 4, and 5 for glassy *o*-terphenyl, 1-methylnaphthalene, and decalin, respectively. One can see a progressive narrowing of the $^3C_{60}$ EPR spectrum with the temperature increase. Qualitatively, this narrowing looks very similar for the all glasses studied.

Previously, for interpreting the temperature variation of the EPR spectra of $^3C_{60}$, the concept of rapid pseudorotation (dynamic Jahn−Teller effect) was used.[4−7] To influence the EPR line shape, the exchange rate, R, must be comparable to or higher than the EPR line width $\Delta\omega$, $R \geq \Delta\omega \sim D/\hbar \approx 2 \times 10^9$ rad/s. In the case of fast isotropic pseudorotation, $R \gg \Delta\omega$, the ZFS interaction is effectively averaged to zero, which leads to the collapse of the triplet spectrum into a narrow single line. Such a line was observed for $^3C_{60}$ in liquid solutions by TR EPR[4,7] and FT EPR.[19]

The model of the $^3C_{60}$ pseudorotation with the intermediate exchange rate, $R \sim \Delta\omega$, was used for explaining the temperature variation of the $^3C_{60}$ EPR spectrum in glassy toluene.[7] The correlation time $\tau_c \sim R^{-1}$ of the stochastic $\pi/2$ jumps of the principle z axis of the ZFS tensor was varied in simulations within the limits of 0.03−5 ns, which provided the temperature variation of the EPR line shape that was in reasonable agreement with experiment. However, in the case of intermediate exchange, the transversal spin relaxation time T_2 must be on the order of τ_c.[28] This implies very short T_2, which definitely would make impossible the echo signal observation because of the dead time problem. Note that in ref 7, the time-resolved EPR was used, instead of ESE as in our case. In the present work, we observed T_2 larger than 100 ns for the entire temperature ranges studied (see below). Therefore, we conclude that the intermediate exchange model is not consistent with our experimental data.

To explain the whole set of our experimental observations, we suggest that pseudorotation is fast, $R \gg \Delta\omega$, and anisotropic,

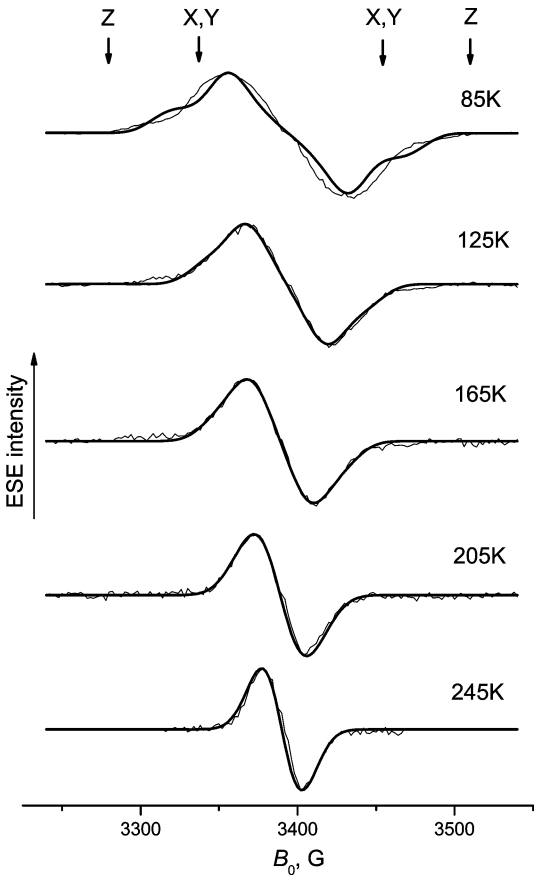

Figure 3. Thin lines: the experimental echo-detected EPR spectra of $^3C_{60}$ in *o*-terphenyl glass at different temperatures measured at τ = 120 ns. Thick lines: simulated spectra (see text). Spectra are arbitrarily shifted along the vertical axis. The arrows mark the field position corresponding to the canonical orientations of $^3C_{60}$ in the absence of motion.

occurring in a potential created by the interaction of the distorted fullerene molecule with the glassy matrix. (The anisotropy of the matrix cage around the fullerene molecule naturally follows from the disordered character of the glass.) Fast pseudorotation in this potential leads to only partial averaging of ZFS and therefore to partial narrowing of the EPR line shape. The temperature dependence of the line shape in this model may appear because of the increasing accessibility of different orientations when the temperature increases.

We assume that this local potential is axially symmetric. The direction of the local matrix symmetry axis in the ensemble of $^3C_{60}$ molecules is randomly distributed with respect to the external magnetic field. Then, in our model, also the axial symmetry of the ZFS of $^3C_{60}$ is assumed (i.e., $E = 0$), which is in agreement with data for $^3C_{60}$ in toluene glass.[14] Therefore, the local potential U may be expressed as a function of a single angle α between the local symmetry axis and the principal z axis of the molecular framework, and $U = U(\alpha)$. The resulting EPR line shape can be calculated by employing statistical averaging over α, with the probability density $dW/d\alpha$ determined by Boltzmann distribution

$$\frac{dW}{d\alpha} = \exp\left(-\frac{U(\alpha)}{kT}\right) \cdot \sin\alpha \qquad (9)$$

where k is the Boltzmann constant and T is temperature.

Let us introduce one more framework (x', y', z') that is related to the local surrounding of the fullerene molecule in the matrix. The z' axis of this framework corresponds to the local matrix symmetry axis. In this framework, the direction of the magnetic field is determined by polar and azimuthal angles θ' and φ'. Because of the axial symmetry of the potential, all possible dependences on the azimuthal angle φ' vanish; therefore, $\varphi' = 0$ was kept in our calculations. Let us denote β as the azimuthal angle determining the orientation of the molecular z axis in this framework (the introduced above angle α is the polar angle). Then, the angle θ, which corresponds to the difference between orientations of the molecular z axis and the external magnetic field, may be calculated for each (θ', α, β) set from the relation $\cos(\theta) = \cos(\theta')\cos(\alpha) + \sin(\theta')\sin(\alpha)\cos(\beta)$.

For each θ' value, the averaging of the B_{ZFS} values (eq 8, where $E = 0$) was performed over all possible angles α and β, weighted by eq 9. In this averaging, we assumed that immediately after the triplet creation, the $^3C_{60}$ longer axis occupies the most favorable orientation along the local symmetry axis. Therefore, the polarizations of the EPR transitions were calculated for each θ' with eq 6 for $\alpha = 0$. The averaged $\langle B_{ZFS}\rangle$ values were substituted into eq 7 instead of B_{ZFS}. Initial populations were taken as $p_x = p_y = 1$ and $p_z = 0$.[7,14] In eq 7, the unresolved hyperfine interactions with surrounding nuclei described by function $f(B)$ were taken as the Gaussian function of 15 G fwhh. The isotropic g-value, $g = 1.9996$, was taken as an average of the $^3C_{60}$ principal g-values known from high-field EPR data.[17] The simplest form of the potential $U(\alpha)$ was chosen

$$U(\alpha) = -V\cos(2\alpha) \qquad (10)$$

which presents a first term in a Fourier-series expansion of the potential, with V standing for the amplitude of this term. A similar form of the potential was used for simulating the ordering of the triplet of the fullerene derivative in a liquid crystal.[29] Amplitude V corresponds to the "matrix orienting potential" parameter, and it was assumed to be the same for all cages.

The ZFS parameter D, equal to 115 G in the magnetic field units, was found from fitting spectra in *o*-terphenyl at 85 K (see Figure 3). This value is close to the known literature data[14] and was used also for other molecular glasses.

The simulated spectra are shown as thick lines in Figures 3−5, where also the field positions for canonical x, y, and z orientations are indicated by arrows. Note that spectra are partially averaged even at low temperatures. A good agreement is seen between the experimental and the simulated spectra. A slight discrepancy observed at low temperatures may be explained by the distribution of the ZFS value D in glassy medium, which was not taken into account here.

In Figure 5, weak temperature-independent wings are seen in the experimental spectra, which are not reproduced in simulations. Also, at 130 K, the shoulders outside of the main peaks appear. Very similar spectra were observed in ref 14 in a toluene matrix in the temperature range of 120−170 K, where it was ascribed to the triplet state of the C_{60} dimer. On the basis of this similarity, we ascribe these spectral features to the C_{60} dimer triplet state.

The temperature dependence of the best-fitted values of the "matrix orienting strength" parameter V (in temperature units) is presented in Figure 6 for the three glasses studied. One can see that it decreases with a temperature increase. The V values are close for *o*-terphenyl and 1-methylnaphthalene, which probably may be explained by intermolecular interaction of the fullerene molecule in both cases with the aromatic surrounding. The lower V value for decalin points to the weaker interaction between $^3C_{60}$ and the matrix of nonaromatic molecules.

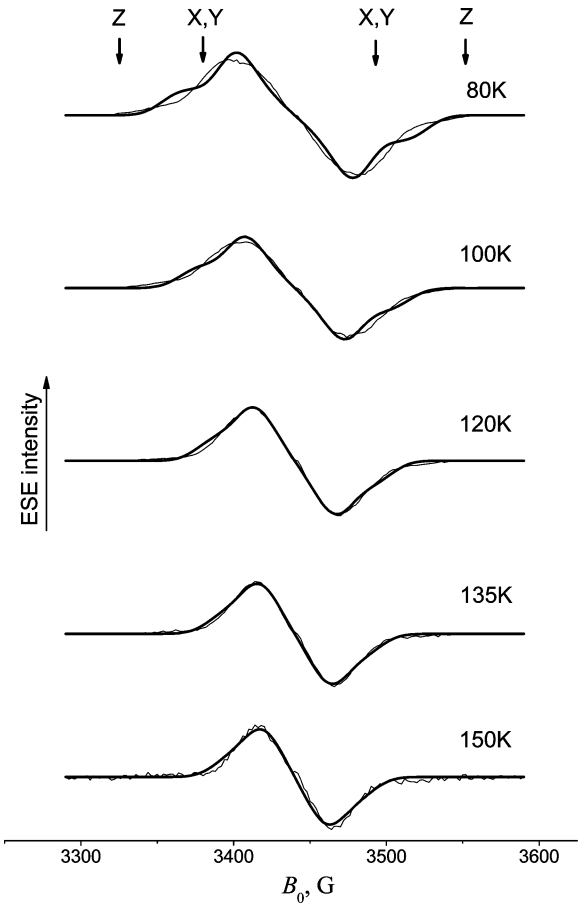

Figure 4. The same as in that Figure 3 for $^3C_{60}$ in 1-methylnaphthalene glass.

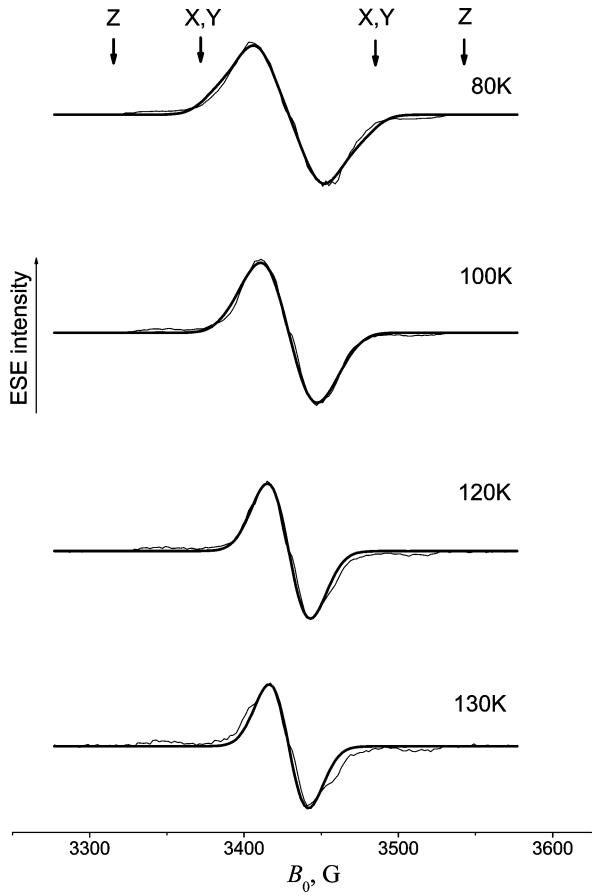

Figure 5. The same as that in Figure 3 for $^3C_{60}$ in decalin glass.

The measured transversal relaxation rates T_2^{-1} for $^3C_{60}$ are given in Figure 7 as functions of temperature. For $^3C_{60}$ in glassy 1-methylnaphthalene and decalin, the sharp increase of the T_2^{-1} temperature dependence near 100 K is seen. For *o*-terphenyl below 240 K, T_2^{-1} only slightly depends on temperature, while above this temperature, a sharp increase of the dependence also occurs. Note that near 100 K, a local maximum of the T_2^{-1} temperature dependence for *o*-terphenyl is seen.

To disentangle the possible contributions to the T_2^{-1} rate of the $^3C_{60}$ pseudorotation and of the matrix motion, the relaxation rates T_2^{-1} for nitroxide **1** were measured in *o*-terphenyl. (This particular type of nitroxide was chosen to avoid the influence of the methyl group rotation on relaxation rates;[30,31] methyl groups are common residues for the majority of types of nitroxides.) As microwave pulses in these measurements were applied at the maximum of the spectrum, which is known to possess only minor anisotropy, the possible influence of motion of the nitroxide itself was minimized. One can see that T_2^{-1} values for nitroxide **1** at all temperatures are substantially smaller than those for $^3C_{60}$, and the increase of the temperature dependence is remarkably smoother and shifted to higher temperatures.

We may assign the difference of the relaxation rates T_2^{-1} for $^3C_{60}$ and nitroxide to the effect of pseudorotation. If motion is fast and purely stochastic, the contribution of the pseudorotation to the transversal relaxation rate T_2^{-1} may be estimated with the Redfield theory[28]

$$T_2^{-1} = \tau_c \langle \Delta\omega^2 \rangle \qquad (11)$$

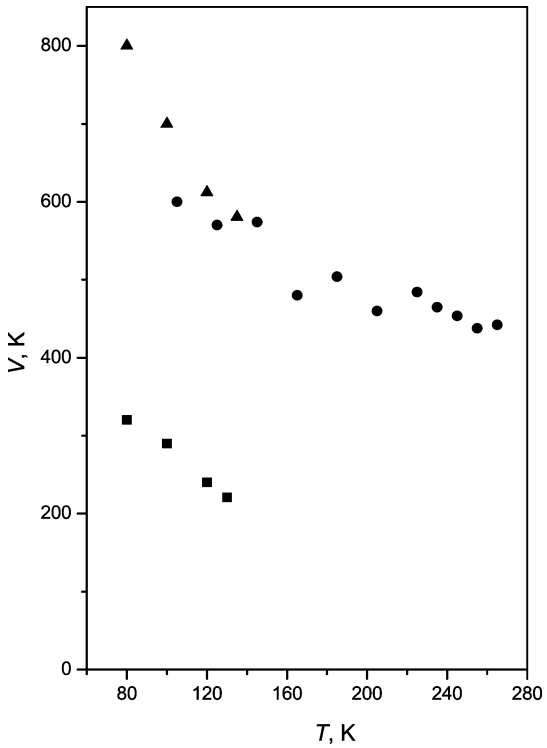

Figure 6. Best-fitted "matrix orienting strength" parameter V in temperature units, obtained from the simulations shown in Figures 3−5 as a function of temperature. Circles: $^3C_{60}$ in *o*-terphenyl glass; triangles: $^3C_{60}$ in 1-methylnaphthalene glass; squares: $^3C_{60}$ in decalin glass.

From data in Figure 7 and using the estimation $\langle \Delta\omega^2 \rangle \sim 4 \times 10^{18}$ rad/s, we obtain $\tau_c \sim 10^{-12}$ s. This is in agreement with

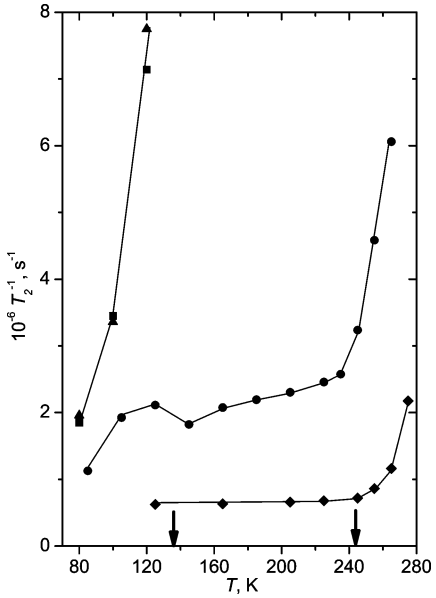

Figure 7. Temperature dependence of the transverse relaxation rate T_2^{-1} for $^3C_{60}$ in different glassy matrices. Circles: *o*-terphenyl glass; triangles: 1-methylnaphthalene glass; squares: decalin glass; diamonds: T_2^{-1} for nitroxide radical **1** in glassy *o*-terphenyl. The lines are drawn to guide the eye. The two arrows mark the temperature of the glass transition for decalin (135 K) and for *o*-terphenyl (243 K).

previous estimations[4] made for the $^3C_{60}$ pseudorotation in liquid solution.

The sharp increase of the T_2^{-1} temperature dependences seen in Figure 7 cannot be related with glass transition. First, glass transition is a macroscopic phenomenon and occurs on the time scale of $\sim 10^3$ s. Second, although for *o*-terphenyl this sharp increase occurs near T_g (243 K), for decalin, this sharp increase takes place near 100 K, which is much lower than T_g (135 K for decalin). The exact T_g value for 1-methylnaphthalene is not known, but it is expected to be close to that of decalin because of the closeness of their melting points in both cases (243 and 230 K, respectively).

The estimated exchange rate, $R \sim \tau_c^{-1} \sim 10^{12}$ s^{-1}, is in the range of frequencies of intermolecular vibrational motions in solids. This prompts us to recognize that pseudorotation may be influenced by the vibrational motions in the surrounding. On the other hand, for glasses, it is known from neutron scattering data and molecular dynamics simulations that above some temperature, the onset of large-amplitude motions of atoms occurs. This is called dynamical transition in glasses. For *o*-terphenyl, it occurs near 240 K.[32,33] For some biological systems, dynamical transition was reported to occur near 100 K.[34,35] Below the "transition" temperature, the mean-squared amplitude of atomic motion, $\langle r^2 \rangle$, linearly depends on temperature, which is ascribed to harmonic oscillations. Above this temperature, the dependence becomes much sharper and strongly nonlinear, which is ascribed to anharmonic[32−35] or stochastic[36] motions. Probably, the increase of the T_2^{-1} temperature dependences seen in Figure 7 may be ascribed to this transition. The onset of the anharmonic or stochastic motions of the matrix molecules may eliminate coupling between the $^3C_{60}$ pseudorotation and vibrational motion in the surrounding, resulting, in this way, in growth of the τ_c value. The latter, according to eq 11, would increase the measured relaxation rate T_2^{-1}.

Note that the T_2^{-1} relaxation rate for nitroxides taken at the spectral shoulders (not at the maximum of the nitroxide EPR spectrum as it is done here) is also sensitive to the dynamical transition in glasses.[37] These studies have shown that the dynamical transition in glasses is related to the motions of molecules as wholes.

The observed increases of the T_2^{-1} temperature dependences for $^3C_{60}$ (Figure 7) are much sharper than the increase of the $<r^2>$ temperature dependence known from neutron scattering and molecular dynamics simulations. Probably, this is because of the time scale of $^3C_{60}$ pseudorotation, which matches better the period of atomic vibrations in solids. It implies that the onset of anharmonic motion occurs in a very narrow temperature interval.

Conclusions

Spin-polarized echo-detected EPR spectra of the excited triplet state of fullerene C_{60} in glassy *o*-terphenyl, 1-methylnaphthalene, and decalin matrices may be interpreted within the model of fast pseudorotation of $^3C_{60}$ in an anisotropic potential, formed by the interaction of the fullerene molecule with the surrounding matrix molecules. (The anisotropy of the matrix cage around the fullerene molecule naturally follows from the disordered character of the glass.) The strength of this potential determined from the numerical simulation of the $^3C_{60}$ EPR spectra depends on the glass and decreases with temperature increase. The correlation time of the pseudorotation, under the assumption that it is a purely stochastic process, is estimated as $\sim 10^{-12}$ s.

The sharp growth of the $^3C_{60}$ transversal relaxation rate T_2^{-1} near 240 K in a glassy *o*-terphenyl matrix may be ascribed to the influence of the dynamical transition from harmonic to anharmonic (or stochastic) vibrational motions known for glasses from neutron scattering and occurring for *o*-terphenyl just near this temperature. The mechanism behind this influence could be eliminating the possible coupling between the $^3C_{60}$ pseudorotation and the vibrational motion of molecules in the surrounding because of the change of the character of motion.

For 1-methylnaphthalene and decalin glasses, neutron scattering data are not available. On the other hand , the temperature of $\sim$100 K, where the sharp growth of the $^3C_{60}$ transversal relaxation rate T_2^{-1} occurs in these glasses, is known as temperature of the dynamical transition in some biological media.[34,35]

This study shows that molecular and spin dynamics of $^3C_{60}$ could serve as a sensitive tool to detect dynamical transition in glassy materials.

Acknowledgment. This work was supported by a grant of the President of Russian Federation for Young Scientists, #MK-7740.2006.3, by the Russian Science Support Foundation, by a joint grant of Russian Foundation for Basic Research and the Japan Society for Promotion of Science, #06-03-91362, by the Grant for Scientific Schools, #6271-2006.3 and by a joint grant of the Russian Foundation for Basic Research and DFG #06-03-04002.

References and Notes

(1) *Optical and Electronic Properties of Fullerenes and Fullerene-Based Materials*; Shinar, J., Vardeny, Z. L., Kafafi, Z. H., Eds.; Marcel Dekker: New York, 2000.

(2) Blank, A.; Kastner, R.; Levanon, H. *IEEE Trans. Microwave Theory Tech.* **1998**, *46*, 2137.

(3) Wasilewski, M. R.; O' Neil, M. P.; Lykke, K R.; Pellin, M. J.; Gruen, D. M. *J. Am. Chem. Soc.* **1991**, *113*, 2774.

(4) Closs, G. L.; Gautam, P.; Zhang, D.; Krusic, P. J.; Hill, S. A.; Wasserman, E. J. *J. Phys. Chem.* **1992**, *96*, 5228.

(5) Terazima, M.; Hirota, N.; Shinohara, H.; Saito, Y. *Chem. Phys. Lett.* **1992**, *195*, 333.

(6) Agostini, G.; Corvaja, C.; Pasimeni, L. *Chem. Phys.* **1996**, *202*, 349.

(7) Regev, A.; Gamiel, D.; Meiklyar, V.; Michaeli, S.; Levanon, H. *J. Phys. Chem.* **1993**, *97*, 3671.
(8) Ceola, S.; Franco, L.; Corvaja, C. *J. Phys. Chem. B* **2004**, *108*, 9491.
(9) Lane, P. A.; Swanson, L. S. *Phys. Rev. Lett.* **1992**, *68*, 887.
(10) Angerhofer, A.; von Schutz, J. U.; Widmann, D.; Muller, W. H.; ter Meer, H. U.; Sixl, H. *Chem. Phys. Lett.* **1994**, *217*, 403.
(11) Wei, X.; Vardeny, V. *Phys. Rev. B* **1995**, *52*, R2371.
(12) Groenen, E. J. J.; Poluektov, O. G.; Matsushita, M.; Schmidt, J.; van der Waals, J. H. *Chem. Phys. Lett.* **1992**, *197*, 314.
(13) Benatti, M.; Grupp, A.; Mehring, M.; Dinse, K. P.; Fink, J. *Chem. Phys. Lett.* **1992**, *200*, 400.
(14) Benatti, M.; Grupp, A.; Mehring, M. *J. Chem. Phys.* **1995**, *102*, 9457.
(15) Benatti, M.; Grupp, A.; Mehring, M. *Synth. Met.* **1997**, *86*, 2321.
(16) van den Berg, G. J. B.; van den Heuvel, D. J.; Poluektov, O. G.; Holleman, I.; Meijer, G.; Groenen, E. J. J. *J. Magn. Reson.* **1998**, *131*, 39.
(17) Dauw, X. L. R.; van den Berg, G. J. B.; van den Heuvel, D. J.; Poluektov, O. G.; Groenen, E. J. J. *J. Chem. Phys.* **2000**, *112*, 7102.
(18) Steren, C. A.; Levstein, P. R.; wan Willigen, H.; Linschitz, H.; Biczok, L. *Chem. Phys. Lett.* **1993**, *204*, 23.
(19) Steren, C. A.; wan Willigen, H.; Dinse, K. P. *J. Phys. Chem.* **1994**, *98*, 7464.
(20) Benatti, M.; Grupp, A.; Bauerle, P.; Mehring, M. *Chem. Phys.* **1994**, *185*, 221.
(21) Surján, P. R.; Udvardi, L.; Németh, K. *J. Mol. Struct.: THEOCHEM* **1994**, *331*, 55.
(22) Surján, P. R.; Németh, K.; Benatti, M.; Grupp, A.; Mehring, M. *Chem. Phys. Lett.* **1996**, *251*, 115.
(23) Visser, J.; Groenen, E. J. J. *Chem. Phys. Lett.* **2002**, *356*, 43.
(24) Van der Waals J. H.; de Groot M. S. *Mol. Phys.* **1959**, *2*, 333.
(25) Wasserman, E.; Snyder, L. C.; Yager, W. A. *J. Chem. Phys.* **1964**, *41*, 1763.
(26) Seidel, H.; Mehring, M.; Stehlik, D. *Chem. Phys. Lett.* **1984**, *104*, 552.
(27) Haufler, R. E.; Conciecao, J.; Chibante, L. P. F.; Chai, Y.; Byrne, N. E.; Flanagan, S.; Haley, M. M.; O'Brien, S. C.; Pan, C.; Xiao, Z.; Billups, I. W. E.; Ciufolini, M. A.; Hauge, R. H.; Margrave, J. L.; Wilson, L. J.; Curl, R. F.; Smalley, R. E. *J. Phys. Chem.* **1990**, *94*, 8634.
(28) Schlichter C. P. *Principles of Magnetic Resonance*; Springer: Berlin, Germant, 1990; Chapter 5.
(29) Bortolus, M.; Ferrarini, A.; van Tol, J.; Maniero, A. L. *J. Phys. Chem. B* **2006**, *110*, 3220.
(30) Tsvetkov, Yu. D.; Dzuba, S. A. *Appl. Magn. Reson.* **1990**, *1*, 179.
(31) Kulik, L. V.; Salnikov, E. S.; Dzuba, S. A. *Appl. Magn. Reson.* **2005**, *28*, 1.
(32) Petry, W.; Bartsch, E.; Fujara, F.; Kiebel, M.; Sillescu, H.; Farago, B. *Z. Phys. B: Condens. Matter* **1991**, *83*, 175.
(33) Tölle, A.; Zimmermann, H.; Fujara, F.; Petry, W.; Schmidt, W.; Schober, H.; Wuttke, J. *Eur. Phys. J. B* **2000**, *16*, 73.
(34) Hayward, J. A.; Smith, J. C. *Biophys. J.* **2002**, *82*, 1216.
(35) Roh, J. H.; Novikov, V. N.; Gregory, R. B.; Curtis, J. E.; Chowdhuri, Z.; Sokolov, A. P. *Phy. Rev. Lett.* **2005**, *95*, 038101.
(36) Fitter, J.; Lechner, R. E.; Dencher, N. A. *J. Phys. Chem. B* **1999**, *103*, 8036.
(37) Dzuba, S. A.; Kirilina, E. P.; Salnikov, E. S. *J. Chem. Phys.* **2006**, *125*, 054502.